Acta Mechanica 181, 91–104 (2006)
DOI 10.1007/s00707-005-0269-4

Acta Mechanica
Printed in Austria

Nonlinear flexural vibrations of layered panels with initial imperfections

C. Adam, Vienna, Austria

Received January 14, 2005; revised May 1, 2005
Published online: November 7, 2005

Summary. In the presented paper the nonlinear response of doubly curved layered panels subjected to time-varying lateral loads is studied. The considered panels are composed of three thick perfectly bonded isotropic layers, which are symmetrically arranged with respect to the middle surface. The structural model utilized to analyze the panels is based on a first-order layerwise theory, which includes transverse shear flexibility, initial geometric imperfections, and Berger-type geometric nonlinearities. The boundaries of panels with polygonal planform are modeled as simply (hard hinged) supported edges with the displacements normal to the edge face fully restrained.

1 Introduction

The nonlinear behavior of imperfect curved panels subjected to lateral loads is a problem, which may be encountered in many civil, mechanical and aerospace engineering applications. A specific area of considerable importance to the advancement of rational design is the development of special-purpose, preliminary design analyses that predict accurately the dynamic response of curved panels made of advanced composite materials. With these analyses a better understanding of the effects of structural parameters, loading conditions and initial geometric imperfections on the response of these panels can be obtained, which could lead to significant increases in structural performance.

The theory of curved plates and panels goes back to Marguerre [1], and it is well known that Marguerre's equations for imperfect panels are fundamentally related to the theory of shallow shells. In spite of the importance of curved layered panels, the literature devoted to moderately large vibrations of initially imperfect panels, composed of several thick layers of different shear flexibility, is not very extensive. This observation is supported by comprehensive review papers for shallow shells by Liew et al. [2] and Qatu [3]. Refs. [4]–[8] are examples of the nonlinear structural vibration analysis of composite panels with initial imperfections. However, it may be important for some applications to represent more accurately effects of layerwise different transverse shear flexibility with the analysis that is used to investigate nonlinear response issues.

In the present paper, a first-order shear theory is applied layerwise to predict the nonlinear dynamic response of shallow doubly curved three-layer sandwich panels of polygonal planform. Flat composite plates with thick layers are treated in a preceding paper [9]. The panel boundaries are modeled as simply supported hard-hinged edges with the displacements perpendicular to the edge face fully restrained. Analyses are based on Berger's plate theory [10]

modified by layerwise application of Mindlin-Reissner kinematic hypothesis. The results illustrate the effects of the interactions that occur between the time-variant mechanical loads, the initial imperfections, and transverse shear flexibility on the nonlinear response characteristics of layered panels.

2 Formulation

2.1 Assumptions and basic equations

Consider a panel composed of three thick isotropic and homogeneous layers in perfect bond. Geometry (layer thickness) and linear elastic properties of the upper and lower face are symmetrically disposed with respect to the middle surface. Faces and core may exhibit extremely different elastic moduli with a common Poisson's ratio v. A small initial geometric imperfection $\hat{w}$ of the middle surface is referenced to the coordinates x and y in the projected xy-plane of the middle surface. Note that the origin ($z = 0$) of the perpendicular coordinate z is the curved middle surface of the panel (and not the xy-plane) [1]. The boundaries of the panel with polygonal planform are modeled as hard hinged supported edges with the displacements perpendicular to the edge face fully restrained. All edges are straight, i.e., the imperfection $\hat{w}$ is zero at the boundaries, and the middle surface of the doubly curved panel and the xy-plane coincide at the edges.

To each layer a first-order shear deformation theory is applied separately, and hence, the displacement field of the i-th layer may be expressed as [11]

$$w_i = w, \quad {}_iu_j = {}_iu_j^{(0)} + z\,{}_i\psi_j, \quad i = 1,2,3, \quad j = x,y. \tag{1}$$

w denotes the displacement component in z-direction common to all layer surfaces, which is superposed to the initial imperfection $\hat{w}$. ${}_iu_x$ and ${}_iu_y$ represent in-plane displacements in the i-th layer in x- and y-direction, respectively, at distance z from the middle surface. ${}_iu_x^{(0)}$ and ${}_iu_y^{(0)}$ denote in-plane displacements at $z = 0$ (see Fig. 1), and ${}_i\psi_x$ and ${}_i\psi_y$ are layerwise cross-sectional rotations, $i = 1,2,3$. Note that the index $i = 2$ refers to quantities of the core, whereas $i = 1, 3$ belong to the upper and lower face, respectively.

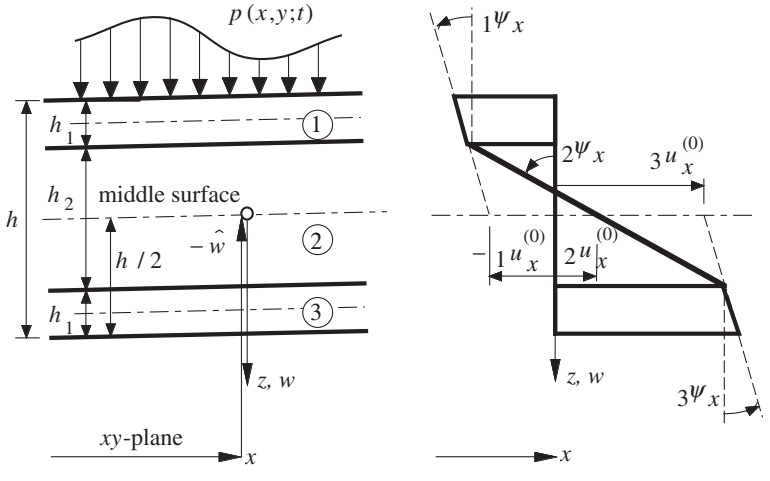

Fig. 1. Imperfect three-layer panel, xz-plane and corresponding horizontal displacement field

The transverse displacement component w is assumed not to be small compared to the panel thickness h, and thus, the interaction between the membrane stresses and the curvatures must be considered. This interaction results in the stretching of the middle surface and subsequently to nonlinear terms in the strain-displacement relations. For moderately large displacements w of a panel with an initial imperfection $\hat{w}$ these nonlinear relations are given by [1]

$$e_j = {}_2u^{(0)}_{j,\,j} + \frac{1}{2}(w,_j)^2 + w,_j\hat{w},_j, \quad e_{xy} = {}_2u^{(0)}_{x,y} + {}_2u^{(0)}_{y,\,x} + w,_x w,_y, \quad j = x, y, \tag{2}$$

where e_x, e_y are the middle surface strains in x- and y-direction, respectively, and e_{xy} denotes the in-plane shear strain. The strains at distance z from the middle surface become

$$ {}_i\varepsilon_j = {}_iu_{j,\,j} + \frac{1}{2}(w,_j)^2 + w,_j\,\hat{w},_j, \quad {}_i\gamma_{xy} = {}_iu_{x,y} + {}_iu_{y,\,x} + w,_x\,w,_y, \quad {}_i\gamma_z = {}_iu_{j,\,z} + w,_j,$$

$$i = 1,2,3, \quad j = x, y. \tag{3}$$

In Eqs. (2) and (3), $(\,)_{,j}$ indicates spatial differentiation of $(\,)$ with respect to j: $\partial(\,)/\partial j$.

The constitutive relations, however, are linear. For an isotropic, elastic material the stress components σ_x, σ_y, τ_{xy} are related to the strains by means of Hooke's law, see, e.g. [12],

$${}_i\sigma_j = \frac{2G_i}{1-v}({}_i\varepsilon_j + v\,{}_i\varepsilon_k), \quad {}_i\tau_{xy} = G_i\,{}_i\gamma_{xy}, \quad i = 1,2,3, \quad j = x, \quad k = y \text{ and } j = y,\ k = x, \tag{4}$$

where G_i is the shear modulus of the isotropic i-th layer. The normal stress component σ_z is assumed to be negligible and thus consequently dropped.

2.2 Interface continuity relations

Assuming perfect bond between the layers (i.e., no interlayer slip is admitted), the in-plane displacements ${}_iu^{(0)}_x, {}_iu^{(0)}_y$ of the faces ($i = 1,\ 3$) can be expressed in terms of the in-plane displacements of the middle surface ${}_2u^{(0)}_x, {}_2u^{(0)}_y$ and the cross-sectional rotations (see Fig. 1):

$${}_iu^{(0)}_j = {}_2u^{(0)}_j + z_i({}_2\psi_j - {}_i\psi_j), \quad i = 1,3,\ j = x, y, \tag{5}$$

where $z_1 = -h_2/Z,\ z_3 = h_2/2$ denote perpendicular distances from the middle surface to the upper and lower interface, respectively.

Transverse shear stress components τ_{xz}, τ_{yz} are specified to be continuous across the interfaces. Two types of approximations are acknowledged in the literature. The "correct" shear stress expressed by means of the law of conservation of momentum satisfies the in-plane equilibrium by itself, see e.g. Yu [11]. Alternatively, prescribing the continuity of the transverse shear stresses according to Hooke's law derives a simplified boundary value problem [13]–[15],

$${}_i\tau_{jz} = G_i({}_i\psi_j + w_j) = {}_{i+1}\tau_{jz} = G_{i+1}({}_{i+1}\psi_j + w_j), \quad i = 1,2,\ j = x, y. \tag{6}$$

In analogy to the Mindlin theory for homogeneous panels Eqs. (6) exhibit the simplified assumption that the shear stress is uniformly distributed throughout the layers. From these relations and in combination with $G_1 = G_3$ it follows that the cross-sectional rotations of both faces are identical,

$${}_1\psi_j = {}_3\psi_j, \quad j = x, y. \tag{7}$$

2.3 Stress resultants of the layered panel

Layerwise stress resultants are determined by integration of the stress components, Eqs. (4), with respect to the thickness of the layers. Utilizing Eqs. (6) and (7) the cross-sectional rotations of the faces are eliminated, and hence, the layerwise resultants can be expressed in terms of the lateral deflection w, the cross-sectional rotations ${}_2\psi_x, {}_2\psi_y$ of the core, the middle surface strains and their derivatives.

The overall stress resultants of the panel are determined by layerwise summation, and the moment resultants m_x, m_y, m_{xy} and shear force resultants q_x, q_y are obtained as [9]

$$m_j = \frac{2}{1-v}\sum_{i=1}^{3}\left\{(\beta_i + C_i){}_2\psi_{j,j} + \beta_i w_{,jj} + v\left[(\beta_i + C_i)\,{}_2\psi_{k,k} + \beta_i w_{,kk}\right]\right\},$$

$$j = x,\ k = y \text{ and } k = x,\ j = y, \tag{8.1}$$

$$m_{xy} = \sum_{i=1}^{3}\left[(\beta_i + C_i)\left({}_2\psi_{x,y} + {}_2\psi_{y,x}\right) + 2\beta_i w_{,xy}\right], \tag{8.2}$$

$$q_j = \delta\left({}_2\psi_j + w_{,j}\right),\ j = x, y. \tag{9}$$

A_i, B_i, C_i and S_i represent layerwise stiffness coefficients:

$$A_i = G_i h_i, \quad B_i = \frac{1}{2}G_i\left(a_{i+1}^2 - a_i^2\right), \quad C_i = \frac{1}{3}G_i\left(a_{i+1}^3 - a_i^3\right), \quad S_i = \kappa^2 G_i h_i,\ i = 1,2,3, \tag{10.1}$$

$$a_1 = -h/2, \quad a_2 = -h_2/2, \quad a_3 = h_2/2, \quad a_4 = h/2, \tag{10.2}$$

and

$$\delta = 2S_1\frac{G_2}{G_1} + S_2, \quad \beta_1 = \beta_3 = \left(\frac{1}{2}B_1 h_2 + C_1\right)\left(\frac{G_2}{G_1} - 1\right), \quad \beta_2 = 0. \tag{11}$$

In S_i a shear correction factor κ^2 is employed, since the transverse shear stresses are assumed to be constant through the thickness. This is the same concept used in the Mindlin-Reissner theories for thick plates. The proper choice of κ^2 is discussed in [11].

The in-plane displacements of the middle surface at the edges Γ are fully restrained, i.e., ${}_2u_x^{(0)}|_\Gamma = 0, {}_2u_y^{(0)}|_\Gamma = 0$ and hence, moderately large lateral displacements may be considered simplified by means of Berger's approximation [10]. This approximation is based on the assumption that the elastic energy given by the second invariant of the middle surface strain tensor may be disregarded as compared to the square of the first invariant without substantially affecting the response. In Berger's approach the influence of the in-plane force resultants is characterized by a time-variant isotropic force n, which is a constant throughout the panel domain Ω. Note that utilizing the higher theory according to Maguerre [1] and von Karman would result in an anistropic in-plane force distribution and subsequently in a more complex set of equations than the presented one. Following a procedure employed by Wah [16] and Irschik [17], n may be related to the lateral deflection w and the initial imperfection $\hat{w}$ by the averaging integral:

$$n = \frac{D}{\Omega}\int_\Omega\left[\frac{1}{2}\left(w_{,x}^2 + w_{,y}^2\right) + w_{,x}\hat{w}_{,x} + w_{,y}\hat{w}_{,y}\right]d\Omega, \quad D = \frac{2}{1-v}\sum_{i=1}^{3}A_i. \tag{12}$$

Equation (12) shows that n is not explicitly affected by the shear [18].

2.4 Equation of motion and boundary conditions

The equation of motion is derived considering the free-body diagram of an infinitesimal panel element, loaded by a lateral forcing function $p(x,y;t)$. Thereby, in a common approximation, both the longitudinal as well as the rotatory inertia are neglected, ${}_i\ddot{u}_j^{(0)} = 0$, ${}_i\ddot{\psi}_j = 0$, thus limiting the analysis to the lower frequency band of structural dynamics.

Conservation of angular momentum with respect to the x- and y-axes and conservation of momentum in x-, y- and z-direction render after some algebra the following equation of motion of the nonlinear panel problem in terms of the lateral deflection w:

$$K\Delta\Delta w + \frac{K}{S_e} n(\Delta\Delta w + \Delta\Delta\hat{w}) - n(\Delta w + \Delta\hat{w}) - \mu\frac{K}{S_e}\Delta\ddot{w} + \mu\ddot{w} = p - \frac{K}{S_e}\Delta p. \tag{13}$$

Expression (13) may be understood as the equation of motion of an imperfect homogeneous shear-deformable panel with mass per unit area μ, effective shear stiffness S_e, and flexural stiffness K. The effective panel properties are given by

$$\mu = 2\rho_1 h_1 + \rho_2 h_2, \quad S_e = \frac{\delta}{\gamma}K, \quad K = \frac{2}{1-v}(2C_1 + C_2), \tag{14.1}$$

with

$$\gamma = \frac{2}{1-v}\left[B_1 h_2\left(\frac{G_2}{G_1} - 1\right) + 2C_1\frac{G_2}{G_1} + C_2\right]. \tag{14.2}$$

In Eq. (14.1), ρ_1 and ρ_2 denote mass densities of the faces and the core, respectively.

The boundary conditions of a composite shear-deformable panel with hard hinged supports can be modeled in the form [15]

$$\Gamma : w = 0, \quad {}_i\psi_s = 0, \quad m_n = 0, \quad i = 1,2,3, \tag{15}$$

where n and s are local Cartesian coordinates at the boundary Γ with the normal n pointing outwards. Furthermore, conservation of momentum in z-direction for a differential panel element at Γ renders

$$\Gamma : q_{n,n} + q_{s,s} + n(\Delta w + \Delta\hat{w}) + p = 0. \tag{16}$$

Considering only polygonal contours Γ (i.e., straight edges): $w = 0$ can be expressed by $w_{,s} = w_{,ss} = 0$, and ${}_i\psi_s = 0$ may be replaced by ${}_i\psi_{s,s} = 0$. Evaluating Eqs. (15) and (16) leads to two boundary conditions in w,

$$\Gamma : w = 0, \quad \Delta w + \frac{1}{S_e} n(\Delta w + \Delta\hat{w}) = -\frac{1}{S_e} p. \tag{17}$$

2.5 Linearized form of the equation of motion and boundary conditions

Linearized lateral vibrations w_l of an imperfect layered panel can be derived from the equation of motion (13) and the corresponding boundary conditions as follows:

$$K\Delta\Delta w_l + \frac{K}{S_e} n\Delta\Delta\hat{w} - n\Delta\hat{w} - \mu\frac{K}{S_e}\Delta\ddot{w}_l + \mu\ddot{w}_l = p - \frac{K}{S_e}\Delta p, \tag{18}$$

$$\Gamma : w_l = 0, \quad \Delta w_l + \frac{1}{S_e} n_l\Delta\hat{w} = -\frac{1}{S_e} p. \tag{19}$$

where n_l denotes the linear part of the spatially uniformly distributed time varying in-plane force resultant n, Eq. (12),

$$n_l = \frac{D}{\Omega}\int_{\Omega}\left(w_{,x}\hat{w}_{,x} + w_{,y}\hat{w}_{,y}\right)d\Omega. \tag{20}$$

3 Solution methodology

The partial differential equation of motion (13) is transformed into a set of ordinary differential equations by series expansions of the initial and superposed dynamic deflection $\hat{w}$ and w, respectively. The employed shape functions must satisfy all boundary conditions. This requirement is achieved by utilizing the ortho-normalized mode shapes $\Phi^{(mn)}(x,y)$ of the corresponding geometric linearized homogeneous shear-deformable panel (i.e., with identical properties, boundary conditions and equally shaped) without imperfection ($\hat{w} = 0$),

$$w(x,y;t) = \sum_{m=1,\,n=1}^{\infty} Y_{mn}(t)\Phi^{(mn)}(x,y), \tag{21.1}$$

$$\hat{w}(x,y) = \sum_{m=1,\,n=1}^{\infty} \frac{\hat{w}_{mn}}{\lambda_{mn}}\Phi^{(mn)}(x,y). \tag{21.2}$$

In Eq. (21.2), λ_{mn} denotes a coefficient ortho-normalizing the *mn*-th mode shape. Substitution of these transformations into Eqs. (12) and (13) and following the procedure of modal analysis leads to a coupled set of ordinary differential equations for the modal coordinates Y_{mn}.

In [19] it has been shown that the mode shapes of a linear shear-deformable shallow shell and of the corresponding plate are identical when the geometry of the shell curvature is affine to one mode shape of the plate. This statement holds true also for the actual problem, because the linearized equation of motion of the imperfect panel, Eq. (18), and that of a geometric linear homogeneous shear-deformable shallow shell can be transferred into each other. Thus, under the assumption that the distribution of the imperfection is proportional to the *kl*-th mode shape,

$$\hat{w}(x,y) = \frac{\hat{w}_0}{\lambda_{kl}}\Phi^{(kl)}(x,y), \tag{22}$$

the modal coordinates Y_{mn} of the nonlinear panel problem are coupled in the following form:

$$\ddot{Y}_{mn} + 2\zeta_{mn}\omega_{mn}\dot{Y}_{mn} + \omega_{mn}^2 Y_{mn} + \frac{D}{\Omega\mu}\alpha_{mn}\frac{\alpha_{kl}}{\lambda_{kl}}\hat{w}_0 Y_{mn}Y_{kl} + \frac{D}{2\Omega\mu}\left(\alpha_{mn}Y_{mn} + \frac{\alpha_{kl}}{\lambda_{kl}}\hat{w}_0\delta_{kl}\right)\sum_{r,s=1}^{\infty}\alpha_{rs}Y_{rs}^2 = \frac{1}{\mu}P_{mn}. \tag{23}$$

In Eqs. (22) and (23), $\hat{w}_0$ represents the amplitude of the imperfection, α_{mn} is the *mn*-th Dirichlet Helmholtz eigenvalue of the corresponding membrane with identical polynomial planform (as the imperfect panel) [20]. ω_{mn} denotes the *mn*-th natural circular frequency of the linearized imperfect layered panel (specified by Eqs. (18) and (19)), [19],

$$\omega_{mn} = \sqrt{\frac{1}{\mu}\left[\frac{KS_e\alpha_{mn}^2}{K\alpha_{mn} + S_e} + \frac{D\hat{w}_0^2\alpha_{kl}^2}{\Omega\lambda_{kl}^2}\delta_{kl}\right]}, \tag{24}$$

and δ_{kl} is the Kronecker delta. Note that only the kl-th frequency is modified by the imperfection proportional to the kl-th mode shape. The mn-th modal load coefficient is determined by

$$P_{mn}(t) = \int_{\Omega} \Phi_{mn}(x,y)\ p(x,y;t) d\Omega. \tag{25}$$

In Eqs. (23), structural damping has been introduced via modal damping coefficients ζ_{mn}. Incorporation of viscous damping in the response is another convenient feature of the modal approach to the nonlinear problem.

4 Nonlinear resonance phenomena of imperfect layered panels

In the following the dynamic response of rectangular panels to time-harmonic excitation is examined. The panels of length a, width b, and thickness h are made of three layers with layer to overall thickness ratios $h_2/h = h_{1(3)}/h = 1/3$. The overall dimension is characterized by the coefficients $a/b = 2/3$ and $h/a = 1/10$. The mechanical properties of the faces and the core are specified through the ratio $G_{1(3)}/G_2 = 20$. Poisson's ratio is selected to be uniform to all layers, $v = 0.3$. A shear coefficient of $\kappa^2 = 1$ is assigned to all panels. Imperfections in form of a sine halfwave are considered,

$$\hat{w}(x,y) = \hat{w}_0 \sin\frac{\pi x}{a} \sin\frac{\pi y}{b}, \tag{26}$$

i.e., they are affine to the fundamental mode shape $\Phi^{(11)}$ of the corresponding flat panel. Thus, the mode shapes of the linearized imperfect and the linearized perfect panel ($\hat{w}_0 = 0$) are identical [19] and given by

$$\Phi^{(mn)}(x,y) = \lambda_{mn} \sin\frac{m\pi x}{a} \sin\frac{n\pi y}{b}, \quad \lambda_{mn} = \frac{2}{\sqrt{ab}}. \tag{27}$$

Note that the x- and y-coordinates point in the direction of length a and b, respectively, and their origin is located in a corner of the panel. In the subsequent examples the influence of imperfections on the nonlinear dynamic response is studied by variation of the ratio $\hat{w}_0/h$.

In particular, nonlinear frequency response functions due to a harmonic distributed lateral forcing function

$$p(x,y;t) = p_0 \sin\frac{\pi x}{a} \sin\frac{\pi y}{b} \cos \upsilon t \tag{28}$$

are derived. Because load p and mode shape $\Phi^{(11)}$ are affine apart from the fundamental modal load coefficient P_{11} all other P_{nm} vanish, compare with Eq. (25),

$$P_{11} = \frac{p_0}{\lambda_{11}} \cos \upsilon t, \quad \text{and } P_{nm} = 0\ \forall\ nm\ \neq 11. \tag{29}$$

For the considered panels loaded by a harmonic distributed lateral forcing function, Eq. (28), higher modes contribute to the static response only when snap-buckling occurs. For the range of parameters where imperfect panels become sensitive to snap-buckling see, e.g. Heuer and Ziegler [21]. In dynamics higher modes due to mode interaction caused by the quadratic and cubic terms become significant for internal resonance.

In the subsequent study it is assumed that the contribution of higher modes to the dynamic response is negligible in the considered frequency range for the selected panel parameters, because $P_{nm} = 0\ \forall\ nm \neq 11$, compare with Eq. (29). Thus, the coupled set of modal equations (23) is reduced to a single nonlinear equation, and the response is assumed to be governed by the fundamental modal coordinate,

$$\ddot{Y}_{11} + 2\zeta_{11}\omega_{11}\dot{Y}_{11} + \omega_{11}^2 Y_{11} + \frac{D\alpha_{11}^2}{2ab\mu}\left(\frac{3\hat{w}_0}{\lambda_{11}}Y_{11}^2 + Y_{11}^3\right) = \frac{1}{\mu}P_{11}, \tag{30}$$

in which

$$\alpha_{11} = \left(\frac{\pi}{a}\right)^2 + \left(\frac{\pi}{b}\right)^2. \tag{31}$$

The linearized fundamental circular frequency ω_{11} is given by Eq. (24) with $nm = 11$, $kl = 11$, and $\Omega = ab$. This single mode assumption is justified later by comparing its outcomes with results from a numerical solution including a coupled multi mode approximation according to Eqs. (23).

Since Eq. (30) includes quadratic and cubic nonlinear terms it is assumed that the steady-state solution for the modal coordinate Y_{11} is composed of a constant term, harmonic and subharmonic terms [22],

$$Y_{11} = d_0 + d_1\cos\upsilon t + d_2\sin\upsilon t + d_3\cos 2\upsilon t + d_4\sin 2\upsilon t. \tag{32}$$

When substituted into Eq. (30) a residual $\bar{q}$ results, and algebraic equations for the constants d_0, d_1, d_3 and d_4 are found by application of Galerkin's rule, see, e.g. the textbooks of Ziegler [12], Cunningham [22] and Sathyamoorthy [23],

$$\int_0^{2\pi/\upsilon} \bar{q}\,\frac{\partial\bar{q}}{\partial d_j}dt = 0, \quad j = 0, 1, 2, 3, 4. \tag{33}$$

The resulting coupled equations for d_0, d_1, d_2, d_3 and d_4 are given in the Appendix.

Figure 2 shows nondimensional frequency response functions of the lateral deflection at the center of a layered panel with an imperfection ratio $\hat{w}_0/h = -0.50$ for a nondimensional load amplitude $p^* = 1.50$. Thereby, p^* is defined as

$$p^* = \frac{p_0 a^3}{K}. \tag{34}$$

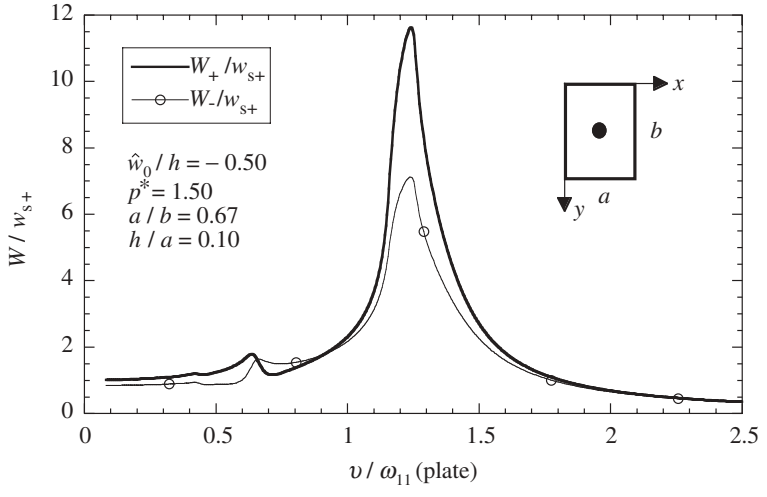

Fig. 2. Nondimensional nonlinear amplitude functions of the lateral deflection at the center of the panel. W_+: steady-state response amplitude in direction of the center of imperfection curvature; W_-: steady-state response amplitude towards the direction of the center of imperfection curvature

Due to the imperfection the amplitude of the steady-state response is different in positive and negative direction with respect to the orientation of the z-coordinate, and the corresponding amplitude functions are denoted by W_+ (positive direction) and W_- (negative direction), respectively. The results W_+ and W_- shown in Fig. 2 are normalized by means of the corresponding static deflection (in positive direction) W_{s+}, and the excitation frequency υ is related to the fundamental frequency ω_{11} of the corresponding linear perfect panel ($\hat{w}_0 = 0$). Viscous damping is considered via a modal damping coefficient of $\zeta_{11} = 0.05$. From this figure it can be seen that the curvature of the panel leads to an approximately 1.2 times larger fundamental primary frequency compared to the fundamental frequency of the corresponding flat panel. The influence of subharmonic resonance can be seen by an additional peak in the response at about half of the primary resonance frequency ($\upsilon/\omega_{11} = 0.6$). In the nondimensional frequency range υ/ω_{11} between 0 and 1.8, W_+ is larger than W_- except for subharmonic resonance. For quasistatic loading the amplitude ratio W_+/w_- is about 1.2, at primary resonance this ratio increases to 1.7. Note that the imperfect panel behaves in the neighborhood of the primary frequency up to a related amplitude W_+/w_{s+} of 7 as a softening spring. However, in the immediate vicinity, where W_+/W_{s+} exceeds 7, the curvature of the resonance curve turns its direction, and the response shows characteristics of a hardening structure.

In Fig. 3, the normalized amplitude function W_+/w_{s+} of the same panel is shown, derived by different approaches. The response amplitude represented by a heavy line is based on the 5 terms approximation of the single modal coordinate Y_{11} according to Eq. (32). In a simplified approach constants d_3 and d_4 are set to zero, and the corresponding frequency dependent steady-state response utilizing the remaining 3 terms of Eq. (32) is displayed in Fig. 3 by a light line. The fat points correspond to the outcomes of time history analyses utilizing the the multi mode approach according to Eqs. (23) in an effort to check the single mode assumption resulting in Eq. (30). Thereby, at time $t = 0$ the time-harmonic load is subjected to the panel, and for each considered discrete excitation frequency the coupled set of equations of motion (23) including 3 modes is solved by direct integration. After decay of the transient response the maximum of the steady-state response is recorded. From Fig. 3, it is obvious that the 5 terms approximation describes the steady-state response with sufficient accuracy, whereas the

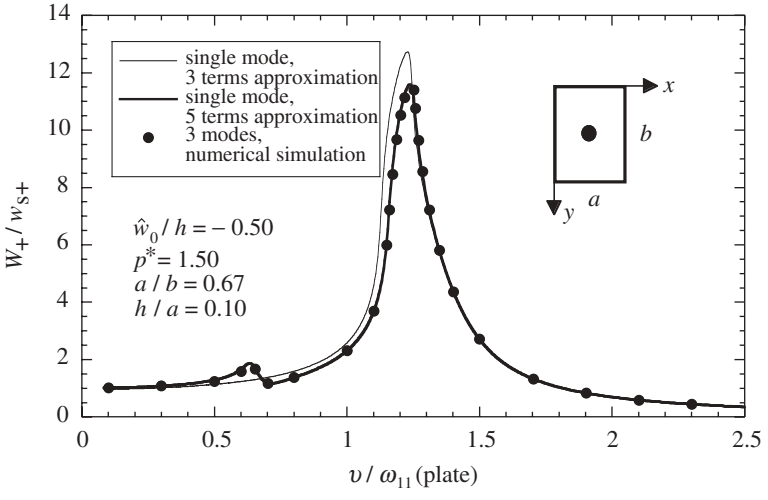

Fig. 3. Nondimensional nonlinear amplitude functions of the lateral deflection at the center of the panel. Different approaches of solution

simplified 3 terms solution is not capable to estimate the peak response accordingly. Thus, all subsequently presented results are based on the 5 terms approximation.

Figure 4 shows the contributions of the constants d_0 to d_4 on the overall steady-state response in order to emphasize their importance at different frequency ratios υ/ω_{11}. As expected outside of the resonance domains the constant d_1 dominates the response amplitude.

Subsequently, the steady-state response behavior of the cross-sectional rotations of the faces and the core is studied. In [7] and [15] it has been shown that for layered beams and plates effective cross-sectional rotations (common to all layers) may be found by equating the overall shear forces of the considered layered structure with the shear force of a corresponding single-layer structure. Effective cross-sectional rotations ${}_e\psi_x, {}_e\psi_y$ can be found also for the actual panel problem. Thereby, the lateral mode shapes $\Phi^{(nm)}$ of series expansion Eq. (21.1) must be replaced by the rotational mode shapes ${}_x\Psi^{(nm)}, {}_y\Psi^{(nm)}$ of the corresponding linear shear-deformable plate problem to render ${}_e\psi_x, {}_e\psi_y$,

$$ {}_e\psi_j(x,y;t) = \sum_{m=1,\, n=1}^{\infty} Y_{mn}(t)\ {}_j\Psi^{(nm)}(x,y), \quad j = x, y. \tag{35} $$

In the actual panel problem these series degenerate to a simple multiplication of the fundamental modal coordinate with the fundamental mode shapes ${}_x\Psi^{(11)}$ and ${}_y\Psi^{(11)}$ of a rectangular shear-deformable panel, given by (see, e.g. [24])

$$ \begin{aligned} {}_x\Psi^{(11)}(x,y) &= -\frac{\pi}{a}\frac{\lambda_{11} S_e}{S_e + K\alpha_{11}} \cos\frac{\pi x}{a}\sin\frac{\pi y}{b}, \\ {}_y\Psi^{(11)}(x,y) &= -\frac{\pi}{b}\frac{\lambda_{11} S_e}{S_e + K\alpha_{11}} \sin\frac{\pi x}{a}\cos\frac{\pi y}{b}. \end{aligned} \tag{36} $$

Then, according to [9] the cross-sectional rotations of the core can be derived from the effective cross-sectional rotations as follows:

$$ {}_2\psi_j = \frac{S_e}{\delta}\,{}_e\psi_j - \left(1 - \frac{S_e}{\delta}\right) w_j \quad j = x, y. \tag{37} $$

The cross-sectional rotations of the faces are found by rearranging Eqs. (6),

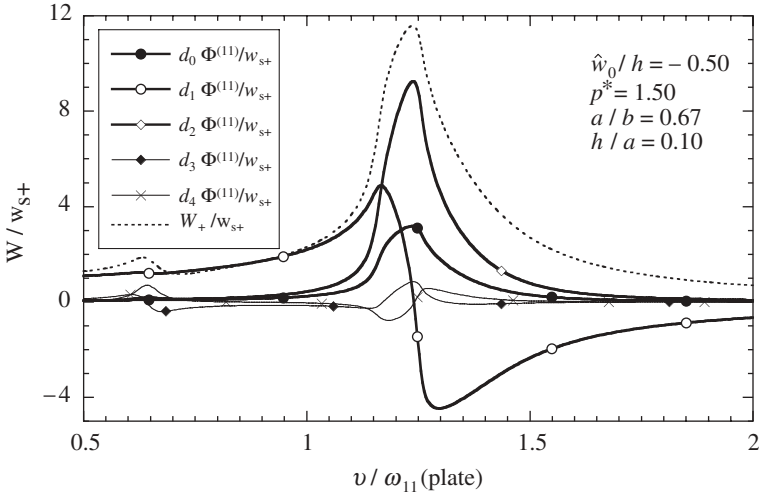

Fig. 4. Contributions of the constants d_0 to d_4 on the overall steady-state response

$$ {}_i\psi_j = \frac{G_2}{G_i}({}_2\psi_j + w_{,j}) - w_{,j}, \quad i = 1,3, \quad j = x,y \tag{38} $$

In Fig. 5, amplitude response functions of the individual cross-sectional rotations about the x-axis ${}_1\psi_x$ and ${}_2\psi_x$, the effective cross-sectional rotation ${}_e\psi_x$ and the derivative of the deflection with respect to $xw_{,x}$ at point ($x/y = 0 / 0.5\ b$) are shown for the considered imperfect panel. The amplitudes of all individual rotations ${}_1\psi_{x+}$, ${}_2\psi_{x+}$, ${}_e\psi_{x+}$, and $W_{,x+}$ are normalized by means of the corresponding static effective cross-sectional rotation ${}_e\psi^s_{x+}$. It can be seen that the cross-sectional rotations of the core and the faces do not coincide, i.e., only a layerwise theory can predict the in-plane deformations appropriately. The amplitude response ${}_1\psi_{x+}$ of the faces and $W_{,x+}$ coincides in a wide range of frequencies, just in the vicinity of the primary response peak $W_{,x+}$ overestimates ${}_1\psi_{x+}$ slightly. Note that the results of Fig. 5 also represent normalized amplitude functions of the cross-sectional rotations about the y-axis ${}_1\Psi_{y+}/{}_e\psi^s_{y+}$, ${}_2\Psi_{y+}/{}_e\psi^s_{y+}{}_e\Psi_{y+}/{}_e\psi^s_{y+}W_{,y+}/{}_e\psi^s_{y+}$ at point ($x/y = 0.5\ a/0$) because length a and b in the denominator of the rotational mode shapes ${}_x\Psi^{(11)}$ and ${}_y\Psi^{(11)}$, respectively, are canceled when the response is normalized.

Finally, the influence of the imperfection to thickness ratio $\hat{w}_0/h$ on the harmonic steady-state response is studied. Figure 6 compares nondimensional amplitude functions W_+ for panels with $w_0/h = 0$, -0.25, -0.50, -0.75 and -1.00 forced by a sinusoidal distributed load with a non-dimensional load amplitude p^* of 1.50. In order to investigate the hardening or softening effect of the imperfection ratio, which becomes visible for large response amplitudes only, the undamped steady-state response is considered, i.e., $\zeta_{11} = 0$. All presented outcomes are related to the corresponding static displacement w_+. In Fig. 6, the hardening effect of increasing ratio $\hat{w}_0/h$ can be seen clearly: the linearized primary frequency (normalized with respect to the linear fundamental frequency of the corresponding plate) is shifted to the right-hand side. In contrast, the normalized nonlinear response amplitude changes its characteristics from a hardening spring to a softening spring with increasing imperfection to thickness ratio $\hat{w}_0/h$. However, when the response of an imperfect panel (see the graph for $\hat{w}_0/h = -0.50$) becomes very large the curvature of the amplitude function changes its direction to a hardening spring behavior.

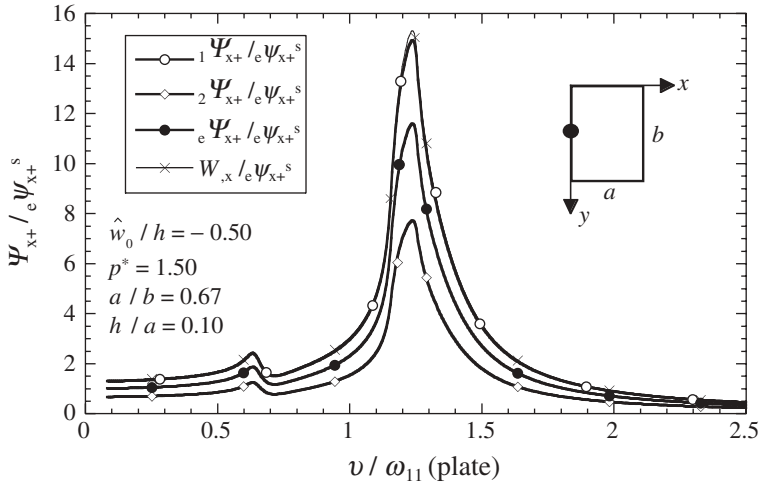

Fig. 5. Nondimensional nonlinear amplitude functions of the layerwise and effective cross-sectional rotations about the x-axis and of the derivation of the deflection with respect to x at ($x/y = 0 / 0.5\ b$)

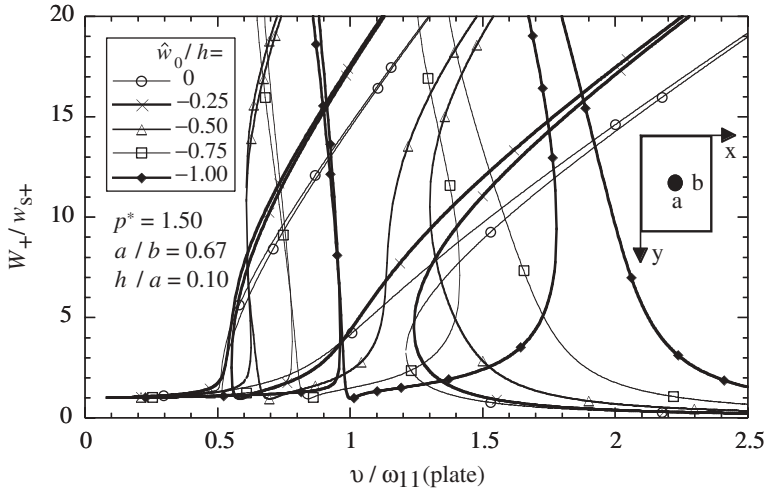

Fig. 6. Nondimensional nonlinear amplitude functions of the lateral deflection at the center of the panel. Undamped response. Variation of the imperfection amplitude ratio $\hat{w}_0/h$

5 Conclusions

The nonlinear dynamic response of imperfect composite panels is analyzed based on a first-order layerwise theory. The layers of the considered structures are symmetrically arranged about the middle surface and possess strongly different shear flexibility. By a simplified formulation of the interface continuity relations this layerwise structural problem is reduced to the lower order of a homogeneous single-layer shear-deformable panel. Geometric nonlinearities of panels with horizontally restrained hard hinged boundaries are considered via Berger's approximation. From the results of rectangular panels with imperfections affine to the linearized fundamental mode shape it can be concluded that the stationary response of the considered structures exhibits layerwise different cross-sectional rotations as main dynamic effect, and thus, a layerwise formulation of the kinematic displacement field is essential for an accurate response prediction. The presented results affirm that initial imperfections and time-harmonic lateral loads interact to change the character of the nonlinear layered panel response. Depending on the ratio of imperfection amplitude to thickness the examined panels show hardening or softening type response behavior, or a combination of both.

Appendix

The following coupled set of nonlinear algebraic equations for the constants d_0, d_1, d_2, d_3 and d_4 and is generated by application of Galerkin's rule:

$$4d_0\omega^2 + 2\left(2d_0^2 + d_1^2 + d_2^2 + d_3^2 + d_4^2\right)c_2 + \left[4d_0^3 + 3d_3\left(d_1^2 - d_2^2\right) + 6d_1d_2d_4 + 6d_0\left(d_1^2 + d_2^2 + d_3^2 + d_4^2\right)\right]c_3 = 0, \tag{A.1}$$

$$4\left[d_1\left(\omega_{11}^2 - \upsilon^2\right) + 2d_2\zeta_{11}\upsilon\omega_{11}\right] + 4(2d_0d_1 + d_1d_3 + d_2d_4)c_2 + 3\left[d_1\left(4d_0^2 + d_1^2 + 4d_0d_3 + d_2^2 + 2d_3^2\right) + 4d_0d_2d_4 + 2d_1d_4^2\right]c_3 = 4p_0/(A_{11}\mu), \tag{A.2}$$

$$4\left[d_2\left(\omega_{11}^2-\upsilon^2\right)+2d_1\zeta_{11}\upsilon\omega_{11}\right]+4(2d_0d_2-d_2d_3+d_1d_4)c_2$$
$$+3\left[d_2\left(4d_0^2+d_1^2-4d_0d_3+d_2^2+2d_3^2\right)+4d_0d_1d_4+2d_2d_4^2\right]c_3=0, \tag{A.3}$$

$$4\left[d_3\left(\omega_{11}^2-4\upsilon^2\right)+4d_4\zeta_{11}\upsilon\omega_{11}\right]+2\left(d_1^2+4d_0d_3-d_2^2\right)c_2$$
$$3\left[4d_0^2d_3+2d_0(d_1-d_2)(d_1+d_2)+d_3\left(2d_1^2+2d_2^2+d_3^2+d_4^2\right)\right]c_3=0, \tag{A.4}$$

$$4\left[d_4\left(\omega_{11}^2-4\upsilon^2\right)+4d_3\zeta_{11}\upsilon\omega_{11}\right]+4(d_1d_2+2d_0d_4)c_2$$
$$+3\left[4d_0d_1d_2+d_4\left(4d_0^2+2d_1^2+2d_2^2+d_3^2+d_4^2\right)\right]c_3=0, \tag{A.5}$$

with

$$c_2=\frac{D\alpha_{11}^2}{2\Omega\mu}\frac{3\hat{w}_0}{A_{11}},\quad c_3=\frac{D\alpha_{11}^2}{2\Omega\mu}. \tag{A.6}$$

References

[1] Marguerre, K.: Knick- und Beulvorgänge. In: Neuere Festigkeitsprobleme des Ingenieurs (Marguerre, K., ed.), pp. 229–235. Berlin: Springer 1950

[2] Liew, K. M., Lim, C. W., Kitipornchai, S.: Vibration of shallow shells: A review with bibliography. AMR **50**, 431–444 (1997).

[3] Qatu, M. S.: Recent research advances in the dynamic behavior of shells: 1989–2000, Part 1: Laminated composite shells. AMR **55**, 325–349 (2002).

[4] Fu, Y. M., Chia, C. Y.: Multi-mode nonlinear vibration and postbuckling of anti-symmetric imperfect angle-ply cylindrical thick panels. Int. J. Non-Linear Mech. **24**, 365–381 (1989).

[5] Bhimaraddi, A.: Nonlinear free vibration analysis of composite plates with initial imperfections and in-plane loading. Int. J. Solids Struct. **25**, 33–43 (1989).

[6] Kapania, R. K., Byun, C.: Vibrations of imperfect laminated panels under complex preloads. Int. J. Non-Linear Mech. **27**, 51–62 (1992).

[7] Heuer, R., Ziegler, F.: Nonlinear resonance phenomena of panel-type structures. Comput. Struct. **67**, 65–70 (1998).

[8] Librescu, L., Nemeth, M. P., Starnes, J. H. Jr, Lin, W.: Nonlinear response of flat and curved panels subjected to thermomechanical loads. J. Thermal Stresses **23**, 549–582 (2000).

[9] Adam, C.: Moderately large flexural vibrations of composite plates with thick layers. Int. J. Solids Struct. **40**, 4153–4166 (2003).

[10] Berger, H. M.: A new approach to the analysis of large deflection of plates. J. Appl. Mech. **22**, 465–472 (1955).

[11] Yu, Y.-Y.: Vibrations of elastic plates. New York: Springer 1995.

[12] Ziegler, F.: Mechanics of solids and fluids, 2nd reprint of 2nd ed. New York: Springer 1998.

[13] Yan, M.-J., Dowell, E. H.: Governing equations for vibrating constrained-layer damping sandwich plates and beams. J. Appl. Mech. **39**, 1041–1046 (1972).

[14] Heuer, R.: Static and dynamic analysis of transversely isotropic, moderately thick sandwich beams by analogy. Acta Mech. **91**, 1–9 (1992).

[15] Adam, C.: Dynamic analysis of isotropic composite plates using a layerwise theory. Compos. Struct. **51**, 427–437 (2001).

[16] Wah, T.: Large amplitude flexural vibration of rectangular plates. Int. J. Mech. Sci. **5**, 425–438 (1963).

[17] Irschik, H.: Large thermoelastic deflections and stability of simply supported polygonal panels. Acta Mech. **59**, 31–46 (1986).

[18] Wu, C.-I., Vinson, J. R.: Influences of large amplitudes, transverse shear deformation, and rotatory inertia on lateral vibrations of transversely isotropic plates. J. Appl. Mech. **36**, 254–260 (1969).

[19] Hochrainer, M., Pichler, U., Irschik, H.: Membrananalogie für Eigenfrequenzen flacher Schalen (in German). ZAMM **79(S2)**, S409–S410 (1999).
[20] Irschik, H.: Membrane type eigenmotions of Mindlin plates. Acta Mech. **55**, 1–20 (1985).
[21] Heuer, R., Ziegler, F.: Thermoelastic stability of layered shallow shells. Int. J. Solids. Struct. **41**, 2111–2120 (2004).
[22] Cunningham, W. J.: Introduction to nonlinear analysis. New York: McGraw-Hill 1958.
[23] Sathyamoorthy, M.: Nonlinear analysis of structures. Boca Raton: CRC Press 1998.
[24] Magrab, E. B.: Vibrations of elastic structural members. Alphen aan den Rijn: Sijthoff and Noordhoff 1979.

Author's address: C. Adam, Center of Mechanics and Structural Dynamics, Vienna University of Technology, Wiedner Hauptstr. 8/E2063, 1040 Vienna, Austria (E-mail: ca@allmech.tuwien.ac.at)